Rev. Téc. Ing. Univ. Zulia. Vol. 39, Nº X, 35 - 40, 2016

Corrosion Behaviour of Heat Treated 1060 Aluminium in Dilute Acid Solutions

Roland Tolulope Loto[1, 2*] and Emilia Ayeoritsenogun Igbogbo[1]

[1]Department of Mechanical Engineering, Covenant University, Ota, Ogun State, Nigeria
[2]Department of Chemical, Metallurgical & Materials Engineering, Tshwane University of Technology, Pretoria, South Africa
**Corresponding author (email: tolu.loto@gmail.com)*

Abstract
The electrochemical corrosion behaviour of untreated, quenched and annealed cold rolled 1060 aluminium specimens was studied through weight loss measurement, potentiodynamic polarization technique and optical microscopy in 0.5, 1, 1.5 and 2M H_2SO_4 and HCl solutions. Data obtained from the tests show that the quenched specimens had the highest corrosion resistance as a result of its hardened surface due to retained saturated solid solution. The untreated aluminium specimens exhibited a lower corrosion resistance than the quenched specimens though the corrosion rates from HCl solution are generally higher than values obtained from H_2SO_4. Annealed specimens had the highest corrosion rate as its passive protective film resulting from the rearrangement of its microstructural constituents could not sustain the aggressive attack of corrosive anions within the acid solution. Micrographs from optical microscopy showed a severely deteriorated annealed morphology resulting from depletion of the grain boundary. Corrosion pits were observed in the untreated specimens while the quenched specimens showed limited deterioration due to general corrosion.

Key words: Corrosion; Quenching; Annealing; Passivation; Acid

1. INTRODUCTION

The Aluminium is an important structural engineering material, its usage ranking only behind ferrous alloys. Its growth in usage and production has continued to increase exponentially (Birbilis *et al*., 2011; Davis, 1999). Aluminium alloys are extensive employed as the material of construction for heat exchangers, aircraft parts, electrical wires, radiators, automotive parts, marine, buildings and architecture, sports equipment and components in water cooling/treatment facilities (Makanjuola *et al*., 2013). The excellent corrosion resistance of aluminium and its application as one of the most versatile commercial used alloy is due to the barrier oxide film that is strongly attached to its surface and when damaged it immediately reforms in some industrial conditions. It is very resistant to corrosion under the majority of service conditions such as seawater, acids and chemical derivatives and no coloured salts are formed to stain adjacent surfaces or discolour products with which it comes into contact. Its light weight, strength and corrosion resistance are some of its most important advantages and the main reasons for its continued application (Sivam *et al*., 2016; Bruhn, 1972; Wernick *et al*., 1987; Bertila *et al*., 2013). Surface deterioration aluminium alloy is usually quite visible due to the formation of whitish precipitates on the alloy surface. Superior mechanical and optimal chemical properties of aluminium alloys are attained as a result of the possible application of structural hardening treatments and compositional modifications (Maria-Cristiana *et al*., 2010). However aluminium alloys are reactive metals and susceptible to electrochemical reactions. The surface film on the alloy is amphoteric and deteriorates significantly when exposed to high concentrations of acids or bases. The subsequent exposure of the substrate alloy after breakdown of the protective film leads to a sequence of electrochemical reactions as the metal continues to deteriorate (Hurlen *et al*., 1984; Mountarlier *et al*., 2005).

Numerous authors have studied the corrosion of aluminium in aqueous environments due to their economic and industrial importance, and a number of theories have been proposed to explain the deterioration of the protective film when anions of corrosive species including chloride diffuse through it into the metal film interface. Some theories propose that the anion chemisorbs on the oxide surface and aids dissolution through the formation of metallic complexes (Lukovits *et al*., 2001; Brett *et al*., 1994; Abedin, 2001; Brett, 1992; Beck, 1988). Solange *et al* (2011) concludes that pitting corrosion of aluminium alloy in saline environment, seems to be closely related to the particles intermetallic second phase and intermetallic composition. Heat treatment is a required process in the final fabrication of any engineering component to make the metal more applicable structurally, mechanically and physically, for some specific application (Rajan *et al*., 1988).

Annealing is a heat treatment process used to change metallic properties such as hardness, toughness etc. through heating of the metal to a specified temperature then slowly cooling it to achieve ductility, softness, removal of internal stresses homogenizing and improvement of cold forming properties. Quenching involves rapid cooling of metal alloy to room temperature to retain the solute in metal solution. This prevents solid-state diffusion and phase precipitation. Quenching results in saturated solution and allows for increased hardness and improved mechanical properties of the metal (Abubakre *et al*., 2009). The 1xxx series of aluminium are strain-hardenable and are applied where strength is not a major consideration but in applications where extremely high corrosion resistance, formability and/or electrical conductivity are required such as in chemical industries. This

research studies the effect of annealing and quenching heat treatment on the electrochemical properties and corrosion resistance of 1060 aluminium alloy in dilute concentrations of H2SO4 and HCl acid media through potentiodynamic polarization, weight loss and optical microscopy.

2. EXPERIMENTAL PROCEDURE

2. 1. Materials

1060 Aluminium (Al 1060) obtained commercially and analysed at the Materials Characterization Laboratory, Department of Mechanical Engineering, Covenant, Ogun State, Nigeria gave an average nominal composition of nominal per cent (%) composition shown as in Table 1. The micrograph for scanning electron microscopy and energy dispersion spectroscopy is shown in Fig. 1.

Table 1. Percentage Nominal Composition of Al 1060

Element Number	Element Symbol	Element Name	Confidence	% Concentration	Error
13	Al	Aluminium	100.0	91.3	0.2
14	Si	Silicon	100.0	4.3	0.8
35	Br	Bromine	100.0	1.9	0.1
6	C	Carbon	100.0	2.5	0.3

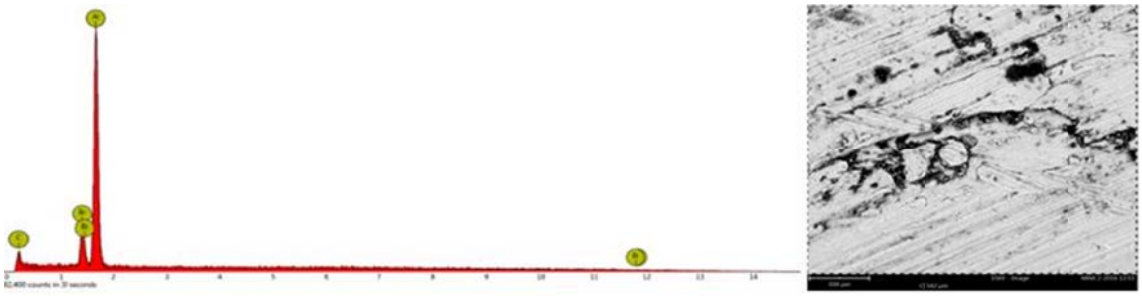

Figure 1. Scanning electron microscopy and energy dispersive spectroscopy micrograph of 1060 Aluminium

2.2. Acid test Solution

Concentrations of 0.5, 1, 1.5 and 2M H_2SO_4 and HCl acid solution at 150 mL were prepared by dilution of an analytical grade of both acids (98% H_2SO_4 and 37% HCl) with distilled water and used as the corrosive test medium.

2.3. Preparation and Heat Treatment of Aluminium Specimens

Al 1060 aluminium rod was machined into 4 test specimens with HSS parting tool on a lathe machine. A 3mm hole was drilled at the center for suspension of the sample in the corrosive media. The average length and diameter of the aluminium is 10 mm x 12 mm The two exposed surface ends of the aluminium specimens were prepared with silicon carbide abrasive papers of 80, 120, 220, 800 and 1000 grits before being polished with 6 µm diamond liquid, rinsed with distilled water and acetone, dried and later stored in a desiccator for weight-loss analysis and potentiodynamic polarization resistance technique in accordance with ASTM G1 - 03(2011) (Schutt and Horvath, 1987). The aluminium specimens were heat treated by annealing in a muffle furnace above the transformation range to 425^{o}C before slowly cooled to 260^{o}C and then gradually to room temperature. This improves the strength and elasticity of the metal. The quenching heat treatment was done at a temperature of 425^{O}C in the muffle furnace after which the samples are removed and immediately quenched in distilled water to achieve the desired metallurgical structure of hardened surface, prevention of low temperature phase transformations and improved mechanical properties while keeping distortion to a minimum. The temperature was regulated using a temperature regulator of accuracy ± 10°C coupled with thermocouple (K-Type) to give the actual sample temperature.

2. 4. Potentiodynamic Polarization Test

Potentiodynamic polarization was performed with the Al 1060 electrodes mounted in acrylic resin with an exposed surface area of 1.13 cm^2 respectively. The aluminium electrodes were prepared according to ASTM G59-97(2014) (Schofield, 2003). The polarization studies were performed at 25^{o}C ambient temperature with Digi-Ivy 2300 potentiostat and electrode cell containing 150 mL of the acid media. Platinum was used as the counter electrode and silver chloride electrode (Ag/AgCl) as the reference electrode. Potentiodynamic measurement was performed from -1.5V to +1.5 V at a scan rate of 0.0016 V/s according to ASTM G102-89(2015) (Charles, 1995). The corrosion current density (j_{corr}) and corrosion potential (E_{corr}) were calculated

from the Tafel plots of potential versus log current. The corrosion rate (γ) and the percentage inhibition efficiency (η_2) were from equation 1.

$$\gamma = \frac{0.00327 \times J_{\text{corr}} \times E_{\text{q}}}{D} \quad (1)$$

where j_{corr} is the current density in μA/cm^2, D is the density in g/cm^3; E_{q} is the specimen equivalent weight in grams. 0.00327 is a constant for corrosion rate calculation in mm/y (Àabanowski, 1997; Brickner, 1968).

2. 5. Weight loss measurement

Weighed steel samples were individually immersed fully into 150 mL of the dilute acid media for 480 h at ambient temperature of 25 ^{o}C. Each sample was removed from the solution at 24 h interval, rinsed with distilled water and acetone, dried and re-weighed according to ASTM G31-12a (Souto *et al*, 2001). Graphical illustrations of corrosion rate, γ (mm/y) versus exposure time T were plotted from the data obtained during the exposure hours. The corrosion rate (γ) calculation is defined as (Antony *et al*, 2007);

$$\gamma = \left[\frac{87.6\tilde{\omega}}{DAT}\right] \quad (2)$$

where $\tilde{\omega}$ is the weight loss in mg, D is the density in g/cm^3, A is the total area in cm^2 and 87.6 is a constant.

2.6. Optical microscopy Characterization

Optical micrographs of the surface morphology and topography of the heat treated aluminium specimens was studied after weight-loss analysis with the aid of Omax trinocular optical metallurgical microscope at the Physical Metallurgical Laboratory, Covenant University, Ogun state, Nigeria.

3. RESULTS AND DISCUSSION

3.1. Potentiodynamic Polarization

The polarization plots for untreated, annealed and quenched Al 1060 specimens from H_2SO_4 and HCl acid solutions are shown in Figs. 2-4. The results from the polarization scans are presented in Tables 2-5. Generally for all Al 1060 specimens, increase in concentration for both acids results in proportionate increase in corrosion rate. Untreated Al 1060 specimens (Table 2) showed greater corrosion resistance in H_2SO_4 solution compared to specimens from HCl solution. The same phenomenon was observed for the annealed and quenched Al 1060 specimens (Tables 3 & 4). The corrosion rate of the annealed Al 1060 specimens are significantly higher than the untreated samples. The non-metallic constituents of annealed Al 1060 precipitate and diffuse from solid solution to concentrate at the grain boundaries, small voids, on undissolved particles, at dislocations, and other imperfections in the aluminum lattice. The changes in Al 1060 during solution annnealing has a detrimental effect on the corrosion resistance of the metal at all concentrations studied. During annealing heat treatment process, the rearrangements of the metallic constituents is responsible for texture development, grain size and mechanical and surface properties which invariably influence the electrochemical behaviour of the annealed Al 1060 specimens. Quenched Al 1060 generally exhibited slightly higher corrosion resistance than the untreated and annealed Al 1060 specimens. The corrosion behaviour of the quenched specimens was significantly influenced by changes in their metallurgical structure. The difference in their intermetallic particles, their sizes and frequency of precipitation determine their overall microstructure and response to attack from chlorides and sulphates ions, however the overall effect of quenching heat treatment on the corrosion resistance of Al 1060 is minimal (Slamova *et al*., 2000). Quenching results in a saturated solid solution responsible for a hardened metal, previous research has shown that the highest degree of corrosion resistance is through quenching (Van Horn, 1967). The presence of chloride and sulphate ions significantly influence the corrosion behaviour of Al 1060 specimens due to their ability to react with and penetrate into the protective oxide film, thereby breaking its passivity under induced potential during potentiostatic scanning (Sato, 1987). Corrosion potential values for Al 1060 specimens in HCl are much higher than values in H_2SO_4 solution. There is a significant negative shift in corrosion potential values for Al 1060 specimens in HCl acid solution for untreated, annealed and quenched specimens. Similar phenomenon was observed by Caperali et al (2008) which implies deterioration of the passive aluminium oxide layer on the specimens and removal of chloride/aluminium compounds on the metal surface according to the equation (Khaled, 2010):

$$Al^{3+}(\text{crystal oxide}) + 2Cl^{-} + 2OH^{-} \rightarrow Al(OH)_2Cl^{-}_2. \quad (3)$$

The small size of Cl^{-} ions enables penetration through the passive oxide film under the effect of an electric field to maintain electrical neutrality and hydrolysis of the corrosion products causing acidification, and hence prevents repassivation. The accumulated presence of corrosive ions within the acid solution accelerated the corrosion rate of all Al 1060 specimens after 0.5 M acid concentration due to destruction of the passive oxide layer that forms on the metal surface. The passive layer consist of different modification of the oxide Al_2O_3,

hydroxide $Al(OH)_3$, or the oxyhydroxide AlOOH (→passivity). In the acid solution Al 1060 dissolves to Al^{3+} ions according to the following reaction

$$Al \rightarrow Al^{3+} + 3^{e-} \quad (4)$$

The oxide layers dissolves and Al^{3+} ions are formed according to equation (5)

$$Al(OH)_{3(aq)} + 3H^{+} \rightarrow Al^{3+}{}_{(aq)} + 3H_2O \quad (5)$$

Increase in corrosion current density observed on the plot is as a result of active metal dissolution reaction of the passive film. The anodic and cathodic Tafel slope of the annealed and quenched Al 1060 specimens did not showed any noticeable change despite the changes in their metallurgical structure, however the cathodic reactions tend to predominate over the anodic suggesting that the mechanism of the dissolution process is majorly through hydrogen evolution due to aluminium ion hydrolysis according to the equation;

$$2H^{+} + 2e^{-} \rightarrow H^{2} \quad (6)$$

The interaction between local cathodes, anodes and the metal substrate leads to the uniform corrosion of Al 1060 specimens. The protective oxide layer represents the thermodynamic stability of Al 1060 specimens in the corrosive environment - acting as a physical barrier as well as being capable of repairing itself in oxidizing environments when damaged. The soluble complex ion formed by the anionic species leads to the dissolution of the metal. (Sato, 1990; Szklarska-Smialowska, 2002). The susceptibility of these alloys is strongly affected by heat treatments, which change the microstructure of the alloy.
formation.

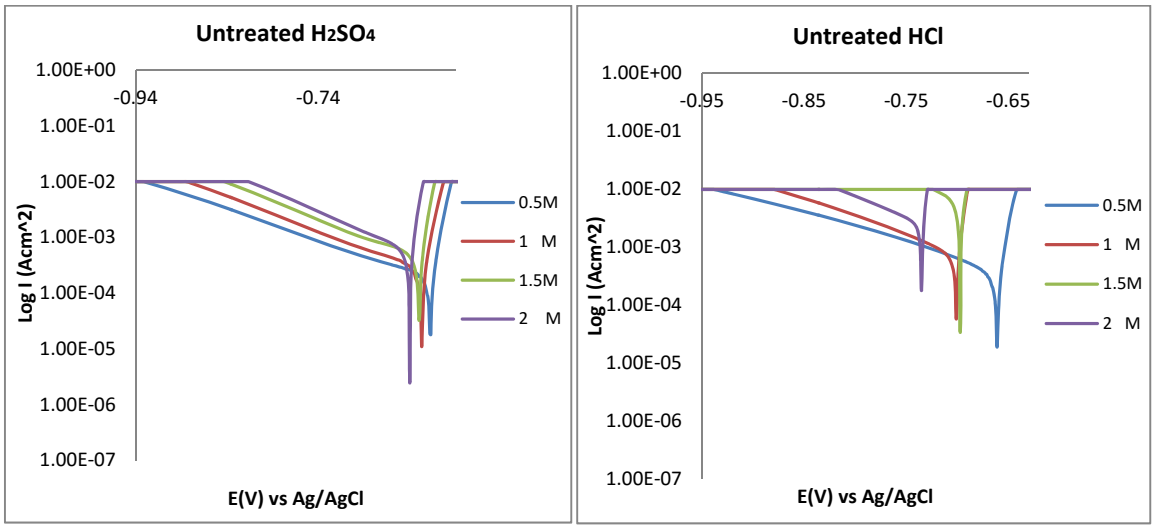

Figure 2. Polarization plots for untreated Al 1060 specimens in 0.5-2M H_2SO_4 & HCl acid media

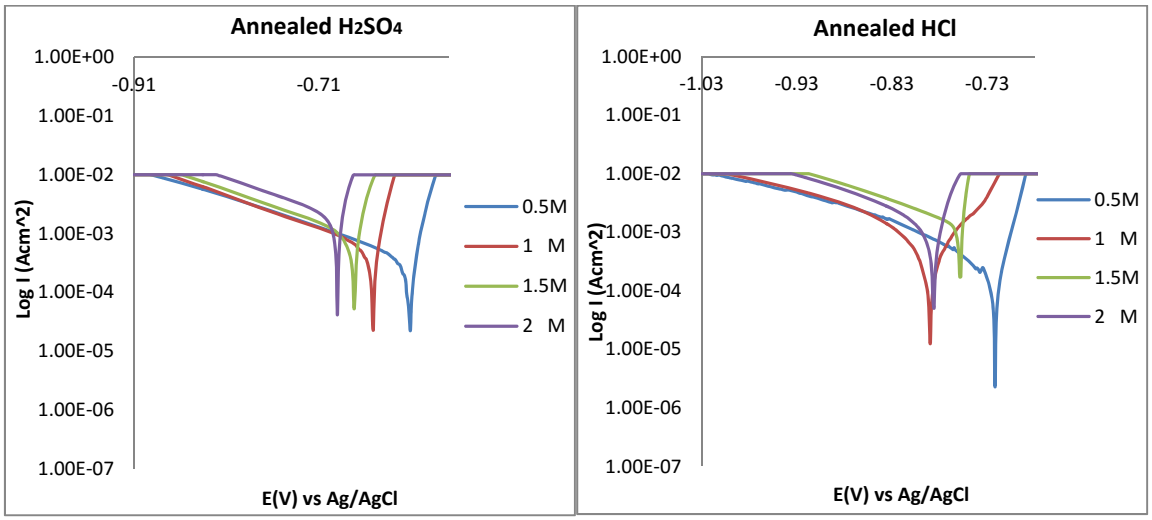

Figure 3. Polarization plots for annealed Al 1060 specimens in 0.5-2M H_2SO_4 & HCl acid media

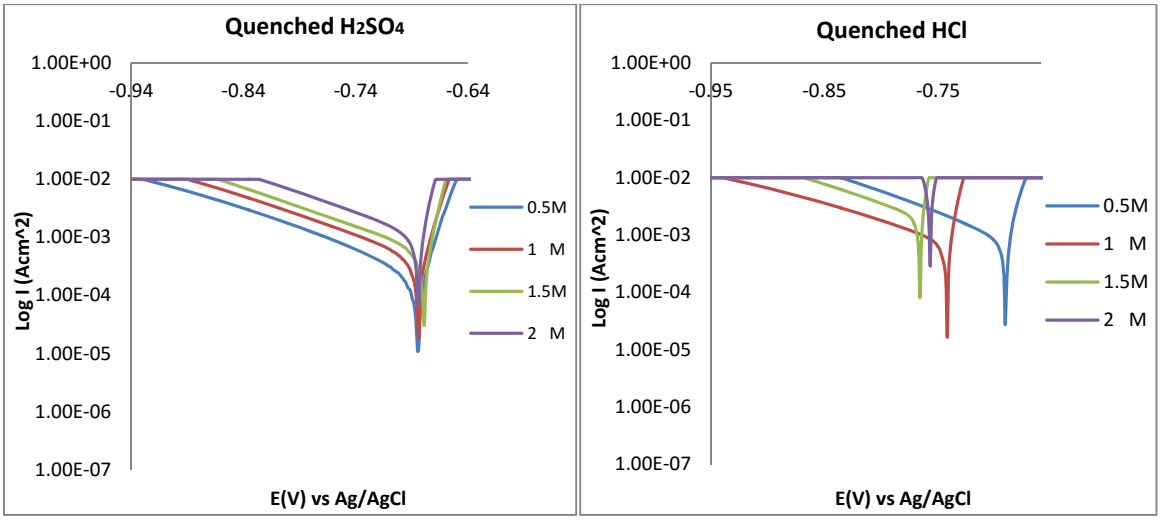

Figure 4. Polarization results for quenched Al 1060 specimens in 0.5-2M H_2SO_4 & HCl acid media

Table 2. Polarization results for untreated Al 1060 specimens in 0.5-2M H_2SO_4 & HCl acid media

Untreated H_2SO_4							
Acid Concentration (M)	**Corrosion Rate (mm/y)**	**Corrosion Current (A)**	**Corrosion Current Density (A/cm²)**	**Corrosion Potential (V)**	**Polarization Resistance, Rp (Ω)**	**Cathodic Tafel Slope (V/dec)**	**Anodic Tafel Slope (V/dec)**
0.5	9.25	9.60E-04	8.50E-04	-0.617	17.6	-5.15	-8.23E-16
1	14.36	1.49E-03	1.32E-03	-0.627	17.24	-5.74	1.65E-15
1.5	20.91	2.17E-03	1.92E-03	-0.630	8.12	-6.24	8.23E-16
2	35.94	3.73E-03	3.30E-03	-0.640	5.21	-7.42	-1.65E-16
Untreated HCl							
Acid Concentration (M)	**Corrosion Rate (mm/y)**	**Corrosion Current (A)**	**Corrosion Current Density (A/cm²)**	**Corrosion Potential (V)**	**Polarization Resistance, Rp (Ω)**	**Cathodic Tafel Slope (V/dec)**	**Anodic Tafel Slope (V/dec)**
0.5	23.51	2.44E-03	2.16E-03	-0.661	10.52	-5.88	-1.65E-15
1	35.36	3.67E-03	3.25E-03	-0.701	2.96	-6.49	0.00E+00
1.5	54.92	5.70E-03	5.04E-03	-0.697	1	0	0.00E+00
2	96.35	0.01	8.85E-03	-0.735	1.2	-5.75	0.00E+00

Table 3. Polarization results for annealed Al 1060 specimens in 0.5-2M H_2SO_4 & HCl acid media

Annealing H_2S0_4							
Acid Concentration (M)	**Corrosion Rate (mm/y)**	**Corrosion Current (A)**	**Corrosion Current Density (A/cm²)**	**Corrosion Potential (V)**	**Polarization Resistance, Rp (Ω)**	**Cathodic Tafel Slope (V/dec)**	**Anodic Tafel Slope (V/dec)**
0.5	27.17	2.82E-03	2.50E-03	-0.611	19.41	-5.5	-1.65E-15
1	39.50	4.10E-03	3.63E-03	-0.651	11.15	-5.3	0.00E+00
1.5	45.67	4.74E-03	4.19E-03	-0.672	6.88	-5.38	1.65E-15
2	73.42	7.62E-03	6.74E-03	-0.690	3.37	-5.44	1.65E-15
Annealing HCl							
Acid Concentration (M)	**Corrosion Rate (mm/y)**	**Corrosion Current (A)**	**Corrosion Current Density (A/cm²)**	**Corrosion Potential (V)**	**Polarization Resistance, Rp (Ω)**	**Cathodic Tafel Slope (V/dec)**	**Anodic Tafel Slope (V/dec)**
0.5	45.24	4.70E-03	4.15E-03	-0.722	36.96	-7.38	1.65E-15
1	56.05	5.82E-03	5.15E-03	-0.790	31.44	-6.97	1.08E+01
1.5	70.72	7.34E-03	6.50E-03	-0.759	1.92	-5.72	0.00E+00
2	108.69	1.13E-02	9.98E-03	-0.786	7.84	-6.29	-1.65E-15

3. 2. Weight loss Measurement

Results obtained from weight loss analysis for weight loss ($\tilde{\omega}$) and corrosion rate (γ) of untreated, annealed and quenched Al 1060 specimens from H_2SO_4 and HCl acid solutions are presented in Tables 5 & 6. Fig. 4, 5 & 6 shows the graphical plot of corrosion rate versus exposure time for Al 1060 specimens in the acid media. Following the trend from potentiodynamic polarization tests, Al 1060 specimens corroded proportionately with increase in concentration of the acid media. Aluminium being an amphoteric metal reacts spontaneously to the changing properties of its protective oxide especially at sites of flaws, non-metallic inclusions, defects etc. The oxide do not offer sufficient protection against aggressive anions of chlorides and and sulphates as a result dissolution of Al 1060 substrate occurs in the acid solution. The dissolution reactions in the presence of the oxide film occurs through movement of Al 1060 ions through the film and an indirect metal dissolution reaction by consecutive oxide film formation and dissolution (Moon and Pyun, 1998; Moon and Pyun, 1999).

Table 4. Polarization results for quenched Al 1060 specimens in 0.5-2M H_2SO_4 & HCl acid media

Quenching H_2SO_4							
Acid Concentration (M)	**Corrosion Rate (mm/y)**	**Corrosion Current (A)**	**Corrosion Current Density (A/cm^2)**	**Corrosion Potential (V)**	**Polarization Resistance, Rp (Ω)**	**Cathodic Tafel Slope (V/dec)**	**Anodic Tafel Slope (V/dec)**
0.5	5.25	5.45E-04	4.82E-04	-0.685	39.85	-7.68	0.00E+00
1	9.83	1.02E-03	9.03E-04	-0.684	16.86	-6.92	0.00E+00
1.5	17.92	1.86E-03	1.65E-03	-0.679	9.36	-6.62	0.00E+00
2	30.25	3.14E-03	2.78E-03	-0.684	4.18	-6.9	0.00E+00
Quenching HCl							
Acid Concentration (M)	**Corrosion Rate (mm/y)**	**Corrosion Current (A)**	**Corrosion Current Density (A/cm^2)**	**Corrosion Potential (V)**	**Polarization Resistance, Rp (Ω)**	**Cathodic Tafel Slope (V/dec)**	**Anodic Tafel Slope (V/dec)**
0.5	16.86	1.75E-03	1.55E-03	-0.691	5.22	-7.45	0.00E+00
1	30.64	3.18E-03	2.81E-03	-0.742	4.25	-6.18	-1.65E-15
1.5	47.21	4.90E-03	4.34E-03	-0.766	1.41	-6.45	0.00E+00
2	83.83	8.70E-03	7.70E-03	-0.757	0.77	0	0.00E+00

The presence of Cl^- and SO_4^{2-} ions caused an increase in corrosion current densities but slightly affects the corrosion potential. The results show that the aggressiveness of the anions is due to their easy adsorbability onto the surface of the protective oxide film and diffusion through the pores causing the rupture of the protective layer on Al 1060 surface (Belkhaouda *et al*., 2010). Table 5 shows a significant increase in weight loss and corrosion rates for Al 1060 specimens with increase in H_2SO_4 acid concentration. Specimens for annealed Al 1060 specimens showed higher susceptibility to corrosion than the untreated specimens, while quenched Al 1060 showed the lowest corrosion rates in comparison to the untreated and annealed specimens. The same phenomenon was observed in Table 6 for Al 1060 specimens in HCl acid solution, though at higher corrosion rate values. The electrochemical behaviour of the untreated, annealed and quenched Al 1060 specimens from the onset to the end of the exposure period are clearly depicted in the figures earlier mentioned (Figs. 4-6). The figures show that heat treatment has limited effect on the general corrosion behaviour of the Al 1060 specimens. The active passive reaction of the metal varies with exposure time and acid concentration with the exception of the unusual behaviour of Al 1060 specimen in 1.5M H_2SO_4 (Fig. 4).

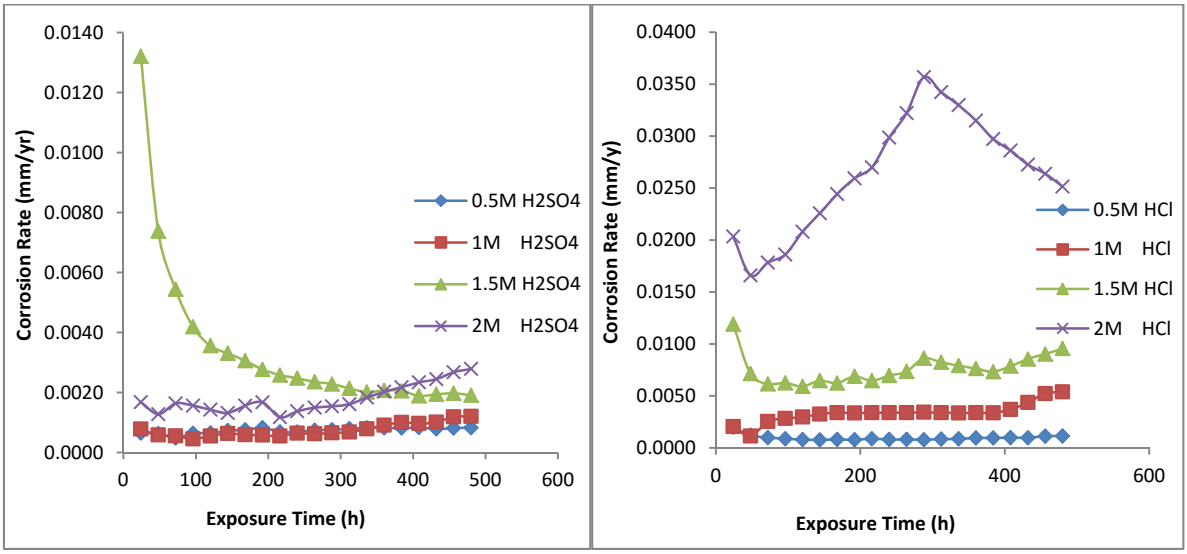

Figure 4. Graphical plot of corrosion rate versus exposure time for untreated Al 1060 specimen in H_2SO_4 & HCl acid media

Table 5. Results for Al 1060 specimens (untreated, annealed and quenched) from H_2SO_4 acid media

		Untreated		**Annealed**		**Quenched**	
Al 1060 Specimens	**H_2SO_4 Conc. (M)**	**Weight Loss (g)**	**Corrosion Rate (mm/yr)**	**Weight Loss (g)**	**Corrosion Rate (mm/yr)**	**Weight Loss (g)**	**Corrosion Rate (mm/yr)**
A	0.5	0.074	0.0008	0.211	0.0017	0.058	0.0006
B	1	0.107	0.0012	0.245	0.0027	0.082	0.0009
C	1.5	0.170	0.0019	0.354	0.0040	0.112	0.0013
D	2	0.249	0.0028	0.685	0.0077	1.133	0.0015

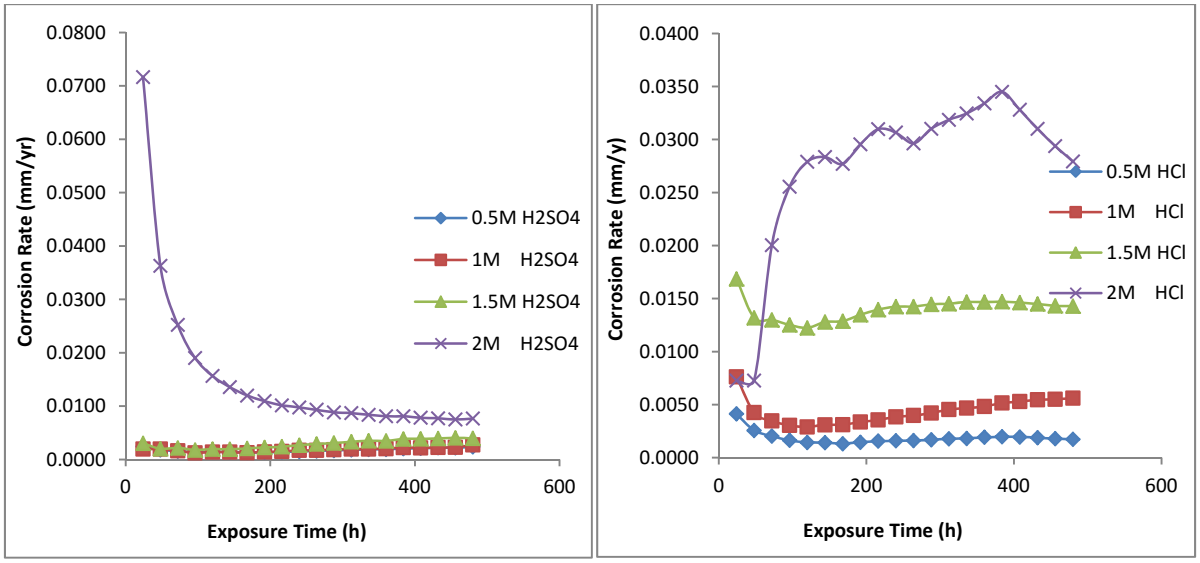

Figure 5. Graphical plot of corrosion rate versus exposure time for annealed Al 1060 specimen in H_2SO_4 & HCl acid media

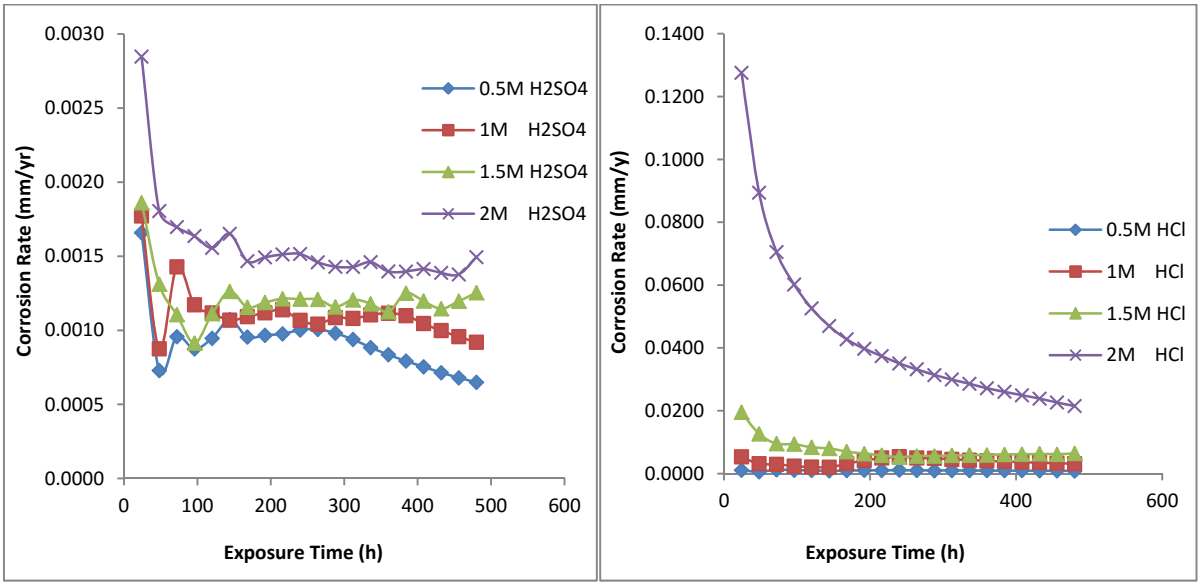

Figure 6. Graphical plot of corrosion rate versus exposure time for quenched Al 1060 specimen in H_2SO_4 & HCl acid media

Table 6. Results for Al 1060 specimens (untreated, annealed and quenched) from HCl acid media

		Untreated		Annealed		Quenched	
Al 1060 Specimens	**HCl Conc. (M)**	**Weight Loss (g)**	**Corrosion Rate (mm/yr)**	**Weight Loss (g)**	**Corrosion Rate (mm/yr)**	**Weight Loss (g)**	**Corrosion Rate (mm/yr)**
A	0.5	0.101	0.0011	0.210	0.0024	0.075	0.0008
B	1	0.481	0.0054	0.501	0.0056	0.280	0.0031
C	1.5	0.852	0.0096	1.275	0.0143	0.573	0.0064
D	2	2.244	0.0252	2.491	0.0279	1.919	0.0215

3.3 Optical Microscopy

The optical micrographs give information about the resulting microstructure of the material before and after heat treatment and corrosion test. The micrograph for the as received, untreated, annealed and quenched Al 1060 specimens from H_2SO_4 and HCl acid solution after the corrosion test are shown in Fig. 7 - Fig. 10. Fig. 7 shows the micrographs of untreated Al 1060 specimen before the corrosion test. The lined surface on the micrograph is due to the effect of machining of the specimens. The micrograph morphology tends to be heterogeneous due to the effect of cold working. The micrograph of the untreated specimen (Fig. 8) after the corrosion test showed the

presence of macroscopic pits on the sample from H_2SO4 acid, this seems to be absent on the specimen from HCl probably because the pits are microscopic due to the action of chloride ions and its high diffusivity. It is also suggested that the pits on the HCl specimens are covered by white or gray powder-like deposits appearing as blotches on the surface (Rudolph, 1961). Fig. 9 shows the morphology of the annealed specimen. It is clearly evident that intergranular corrosion occurred along and adjacent to the grain boundaries while the bulk of the grains were mildly unaffected due to the segregation effects and precipitation of specific phases at the grain boundaries. This phenomenon causes the grain boundary to be largely anodic as against the bulk cathodic substrate of the specimen. The deteriorated morphology is responsible for the high corrosion rate of the annealed specimens as a result of the slow cooling of the specimens' elevated temperature, the impurities and trace alloying elements precipitate and diffuse from solid solution to aggregate at the grain boundaries, small voids, on undissolved particles, at dislocations, and other imperfections in the aluminum lattice (Croucher, 1982). The high rate of heat extraction experienced by the quenched specimen and its higher resistance to corrosion is responsible for its finer microstructure. The hardened surface of saturated solid solution from quenching heat treatment significantly influenced the morphology of the quenched Al specimens (Fig. 10). The quenched surface showed strong resistance to pitting and intergranular corrosion; however it is less immune to general corrosion occurs.

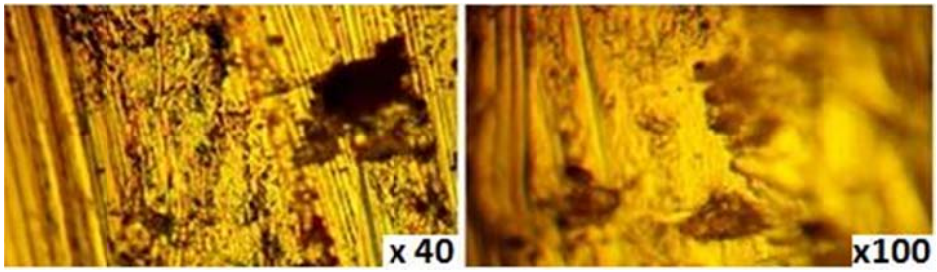

Figure 5. Optical micrographs of untreated Al 1060 specimens before corrosion test

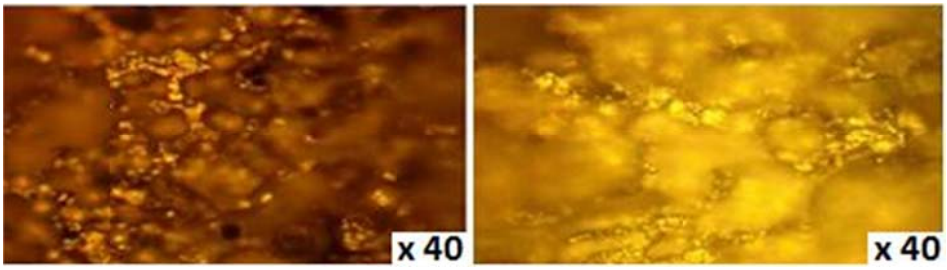

Figure 6. Optical micrographs of untreated Al 1060 specimens in H_2SO_4 and HCl acid after corrosion test

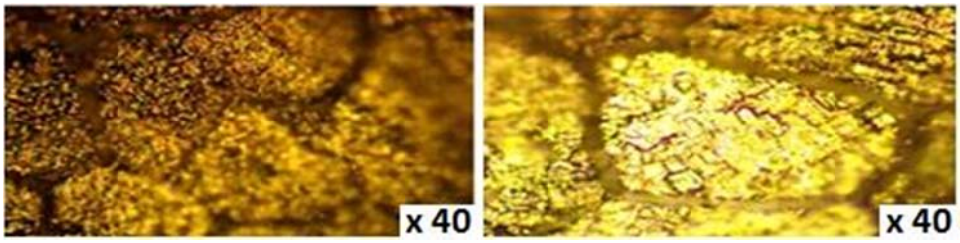

Figure 7. Optical micrographs of annealed Al 1060 specimens in H_2SO_4 and HCl acid after corrosion test

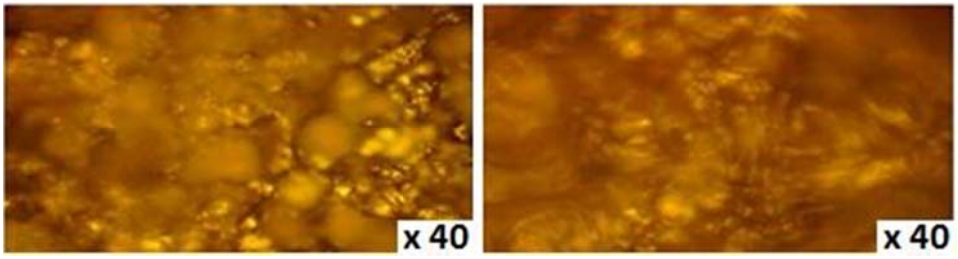

Figure 8. Optical micrographs of quenched Al 1060 specimens in H_2SO_4 and HCl acid after corrosion test

4. CONCLUSION

Quenching heat treatment reduced the corrosion susceptibility of cold rolled 1060 aluminium; the metallurgical structure of hardened saturated solid solution exhibited strong resistance to pitting and intergranular corrosion due to improved passivation properties. The quenched micrograph showed a slightly depleted morphology from general corrosion. Annealed aluminium specimen was observed to be the most susceptible to sulphate and chloride attack leading to intergranular corrosion and severe deterioration along the grain boundaries. Results of corrosion rates from the electrochemical techniques confirms the severity of annealing heat treatment with values much lower than the untreated cold rolled aluminium. Pitting corrosion was observed on the micrographs of the untreated aluminium from HCl solution due to the debilitating action of chlorides.

Acknowledgements

The authors are grateful to the Department of Mechanical Engineering, Covenant University, Ota, Ogun State, Nigeria for the provision of research facilities for this work.

REFERENCES

Àabanowski J (1997) “Duplex stainless steels - new material for chemical industry”, *Apparatus and Chemical Engineering*, 36(2), pp. 3-10.

Abubakre OK, Mamaki UP, Muriana RA (2009) "Investigation of the quenching properties of selected media on 6061 aluminum alloy", *Minerals and Materials Characterization and Engineering*, 8(4), pp. 303-315.

Antony PJ, Chongdar S, Kumar P, Raman R (2007) “Corrosion of 2205 duplex stainless steel in chloride medium containing sulphate-reducing bacteria”, *Electrochimica Acta*, 52, pp. 3985–3994.

Beck TR (1998) “Size distribution of etch pits in aluminium”, *Electrochimica Acta*, 33(10), p. 1321.

Belkhaouda M, Bazzi L, Salghi R, Jbara O, Benlhachmi A, Hammouti B, Douglad J (2010) “Effect of the heat treatment on the behaviour of the corrosion and passivation of 3003 aluminium alloy in synthetic solution”, *Journal of Materials Environmental Science*, 1(1), pp. 25-33

Bertila A, Matilde F, Oladis T, Silagdy A, Melani C, Jomar R, Raúl C (2013) “Corrosion costs in preventive and corrective maintenance in equipment and facilities in industry”, *Revista Tecnica de la Facultad de Ingenieria Universidad Del Zulia* 36(1), 23 - 33

Birbilis N, Muster T, et al. (2011) “Corrosion of aluminum alloys. corrosion mechanisms in theory and practice”, 3rd. Ed., CRC Press, pp. 705-736.

Brett CM (1992) “On the electrochemical behaviour of aluminium in acidic chloride solution” *Corrosion Science*, 33(2), pp. 203-210

Brett CMA, Gomes IAR, Martins JPS (1994) “The electrochemical behaviour and corrosion of aluminium in chloride media. The effect of inhibitor anions”, *Corrosion Science*, 36, pp. 915-923

Brickner KG (1968) “Stainless steel for room and cryogenic temperatures”, *Metals Engineering Quarterly*, 25.

Bruhn EF (1972) “Analysis and design of flight vehicle structures”, Jacobs Publishing Inc., Florida, USA

Caperali S, Fossati A, Lavacchi A, Perissi I, Tolstogou-zov A, Bardi U (2008) “Aluminium electroplated from ionic liquids as protective coating against steel corrosion”, *Corrosion Science*, 50, pp. 53l

Charles J (1995) “Composition and properties of duplex stainless steels”, *Welding in the world*, 36, pp. 89-97.

Croucher T (1982) “Quenching of aluminium alloys: what this key step accomplishes”, *Heat Treating*, 14(5), pp. 20-21

Davis JR (1999) “Corrosion of aluminum and aluminum alloys”, ASM International, Materials Park, Ohio, USA.

El Abedin SZ (2001) “Role of chromate, molybdate and tungstate anions on the inhibition of aluminiumin chloride solutions”, *Journal of Applied Electrochemistry*, 31, pp. 711-718

Hurlen T, Lian H, Odegard OS, Valand TV (1984) “Corrosion and passive behaviour of aluminium in weakly acid solution”, *Electrochimica Acta*, 29, pp. 579-585.

Khaled KF (2010) “Electrochemical investigation and modeling of corrosion inhibition of aluminium in molar nitric acid using simesulphur containing amines”, *Corrosion Science*, 52(9), pp. 2905-2916.

Lukovits I, Kalman E, Zucchi F (2001) “Corrosion inhibitors—Correlation between electronic structure and efficiency”, *Corrosion*, 57, pp. 3-9

Makanjuola O, Kayode O, John O, Samuel O (2013) “Inhibition of aluminium in HCl by amine modified epoxy resin”, *Journal of Materials*, http://dx.doi.org/10.1155/2013/479728

Maria-Cristiana E, Ileana PN, Raluca Z, Alina M, Vasile B (2010) “Influence of heat treatment on microstructure and corrosion behaviour of 7 series Al alloys”, Proceedings of the 2nd International Conference on Manufacturing Engineering, Quality and Production Systems (MEQAPS'10). Constantza, Romania

Moon SM, Pyun SI (1998) "Growth mechanism of anodic oxide films on pure aluminium in aqueous acidic and alkaline solutions", *Journal of Solid State Electrochemistry*, 2, pp. 156–161.

Moon SM, Pyun SI (1999) "The formation and dissolution of anodic oxide films on pure aluminium in alkaline solution", *Electrochimica Acta*, 44, pp. 2445–2454.

Mountarlier V, Gigandet MP, Normand B, Pagetti J (2005) "EIS characterisation of anodic films formed on 2024 aluminium alloy, in sulphuric acid containing molybdate or permanganate species" *Corrosion Science*, 47(1), pp. 937-951.

Rajan TV, Sharma CP, Sharma A (1988) "Heat treatment principles techniques", Rajkarnal Electric Press. India, pp. 142-149.

Rudolph EF (1961) "Corrosion on aircraft, *Sport Aviation*", p 7-8, (http://a.moirier.free.fr/Maintenance/Protection/Corrosion%20on%20aircraft.pdf)

Sato N (1987) "Some concepts of corrosion fundamentals", *Corrosion Science*, 27(5), pp. 421-433

Sato N (1990) "An overview on the passivity of metals", *Corrosion Science*, 31, pp. 1-19

Schofield MJ (2003) "Plant engineer's reference book" Butterworth-Heinemann, Oxford, UK.

Schutt HU, Horvath RJ (1987) "Crude column overhead corrosion problem caused by oxidized sulfur species", Corrosion/87, Paper No. 198 NACE International Houston, TX.

Sivam SP, kumar A, Sathiya K, Rajendrakumar S (2016) "Investigation exploration outcome of heat treatment on corrosion resistance of AA 5083 in marine application", *International Journal of Chemical Sciences*, 14(S2), pp. 453-460

Slamova M, Ocenasek V, Cieslar M, Chalupa B, Merle P (2000) "Differences in structure evolution of twin roll cast AA8006 and AA8011 during annealing", *Materials Science Forum*, pp. 331-337.

Solange PDugarte, Benjamín HP, Rosario ÁG, Mauro BV (2011) "Study of pitting corrosion of the commercial aluminium alloy AA3003 in saline environment", *Revista Tecnica de la Facultad de Ingenieria Universidad Del Zulia,* 34(1), pp. 108 - 123.

Souto RM, Rosca ICM, Gonzales S (2001) "Resistance to localized corrosion of passive films on a duplex stainless steel", *Corrosion*, 57, pp. 195-199

Szklarska-Smialowska Z (2002) "Mechanism of pit nucleation by electrical breakdown of the passive film", *Corrosion Science*, 44(5), pp. 1143-1149.

Van Horn KR (1967) "Aluminium: Properties, physical metallurgy and phase diagrams", American Society of Metals International, Metals Park, Ohio.

Wernick S, Pinner R, Sheasby PG (1987) "The surface treatment of aluminum and its alloys", ASN International Finishing Publications Ltd., Teddington, UK.